SUPPLEMENTAL INFORMATION

SUPPLEMENTAL FIGURE LEGENDS

Figure S1. *pdgfb* and *pdgfrb* expression levels are increased in the VDA by HIF1α

(A) qPCR analysis showed expression of *pdgfrb* and *pdgfba* is significantly upregulated with exposure to the Hif1α agonist DMOG (75uM, 22-36hpf), but related factors are not statistically altered (*p<0.05, **p<0.01, two-tailed t-test, n≥3).

(B) qPCR analysis using FACS-sorted populations from *Tg(flk1:dsRed;cmyb:egfp)* embryos at 48hpf indicated that *pdgfba* and *pdgfrb* are expressed in the vasculature (Flk1:dsRed^{+};cMyb:GFP^{-}) and HSCs (Flk1:dsRed^{+};cMyb:GFP^{+}) as well as unlabeled embryonic tissues (normalized to *tbp*).

(C) qPCR analysis of sorted populations from DMSO or $CoCl_2$ treated embryos showed that *pdgfba* was upregulated by $CoCl_2$ in the endothelium (Flk1^{+};cMyb^{-}), while *pdgfrb* was upregulated in both the endothelium (Flk1^{+};cMyb^{-}) and HSCs (Flk1^{+};cMyb^{+}) (*data shown as fold change in gene expression (normalized to tbp) by $CoCl_2$ relative to DMSO)*.

(D) WISH analysis for *flk1* in embryos treated the pan-PDGFR inhibitor AG1295 or the PDGFRβ selective antagonist DMPQ showed no gross impact of treatment on the trunk vasculature compared to controls at 36hpf (n≥20/condition x 2 replicate clutches).

(E) WISH analysis for *ephrinb2a* in embryos exposed to AG1295 and DMPQ treated showed no difference from controls in arterial identity (n value as in S1D).

(F) Notch activity in the ventral dorsal aorta (VDA) as marked by *gfp* expression in the *Tg(EPV.Tp1CMmu.Hbb:EGFP)* Notch reporter line was reduced with AG1295 treatment compared to controls, but not with DMPQ.

(G) Qualitative phenotypic distribution of embryos from panel S1F (n values as in S1D)

Figure S2. Loss of *pdgfrb* impairs Hif1α-mediated HSPC regulation independent of hemogenic niche formation

(A) Expression of *flk1* was grossly unaffected in the vasculature of embryos injected with *pdgfrb* MO in comparison to sibling controls (n≥20/condition x 2 replicate clutches).

(B) Expression of *runx1;cmyb* was decreased by *pdgfrb* knockdown as determined by WISH.

(C) Qualitative phenotypic distribution of embryos from panel S2B (n value as in S2A).

(D) WISH analysis for *runx1;cmyb* revealed decreased expression in *pdgfrb*$^{um148\ +/-}$ embryos, while *pdgfrb*$^{um148\ -/-}$ embryos were similar to wild-type sibling controls.

(E) Qualitative phenotypic distribution of embryos from panel S2D (n≥20/condition x 4 replicate clutches).

(F) Embryonic exposure to the PDGFRβ-selective inhibitor DMPQ (10μM) during HSC formation (Tx 18-36hpf) blocked the increase in *runx1;cmyb* expression in the VDA observed following $CoCl_2$ exposure.

(G) Qualitative phenotypic distribution of embryos from panel S2F (n value as in S2A).

Figure S3. PDGF-B overexpression increases HSPC production in the VDA and CHT

(A) *In vivo* imaging of *Tg(flk1:dsRed;cmyb:egfp)* embryos indicated that the number of Flk1$^+$;cMyb$^+$ HSPCs (arrowheads) in the VDA was increased at 36hpf in *pdgfb* mRNA-injected embryos.

(B) Absolute counts of Flk1$^+$;cMyb$^+$ HSPCs from embryos in panel S3A (Control: 6±1.5, *pdgfb* mRNA: 10.4±2.2; ***p<0.0001, two-tailed t-test, n≥15/condition).

(C) Overexpression of *pdgfb* increased *cmyb* expression in the CHT at 48hpf.

(D) Qualitative phenotypic distribution of embryos from panel 3D (n≥20 condition x 2 replicate clutches).

(E) Representative images of *Tg(cd41:egfp)* embryos injected with pdgfb mRNA showing increase expression in the CHT.

(F) Absolute cell counts in the CHT of embryos from S3E indicated the number of $CD41^{+}$ HSPCs was increased at 48hpf in embryos injected with *pdgfb* mRNA (Control: 13.1±7.4 cells/CHT, *pdgfb* mRNA: 18.9±9.8, n>35/condition, two-tailed t-test, **p<0.0053).

Figure S4. PDGF-B signaling regulates the expression of inflammatory factors in the VDA

(A) qPCR analysis for inflammatory gene expression in embryos injected with *pdgfb* mRNA showed increased expression of *il1b*, *mmp2*, and *mmp9* (*p<0.05, **p<0.01, two-tailed t-test, n≥3).

(B) qPCR analysis using FACS-sorted populations from Tg(*flk1:dsRed*;*cmyb:egfp)* embryos showed that *il6* and its receptors are primarily expressed in the vasculature ($Flk1^{+}$;$cMyb^{-}$) and HSPCs ($Flk1^{+}$;$cMyb^{+}$) (normalized to *tbp*).

(C) Exposure to the gp130 inhibitor SC-144 (1μM) blocked the ability of *pdgfb* mRNA to increase *runx1;cmyb* expression at 36hpf.

(D) Qualitative phenotypic distribution of embryos from panel S4C (n≥20/condition x 3 replicate clutches).

(E) *il6* overexpression strongly increased *runx1* expression in the VDA at 36hpf.

(F) Qualitative phenotypic distribution of embryos from panel S4E (n≥20/condition x 3 replicate clutches).

Figure S5. Hif1α regulates inflammatory signaling to impact HSPC production

(A) qPCR analysis of FACS sorted populations from DMSO or $CoCl_2$ treated embryos indicated that *il6* and its receptor *il6r* were upregulated by $CoCl_2$ in the endothelium ($Flk1^+$;$cMyb^-$) and in HSPCs ($Flk1^+$;$cMyb^+$) compared to matched control samples (*data shown as fold change in gene expression (normalized to tbp) by $CoCl_2$ relative to that of DMSO controls).*

(B) Exposure to SC-144 (1μM) blocked the ability of $CoCl_2$ to increase *runx1;cmyb* expression in the VDA.

(C) Qualitative phenotypic distribution of embryos from panel S5B ($n \geq 20$/condition x 3 replicate clutches).

SUPPLEMENTAL METHODS

Supplemental Methods Table 1: Morpholino sequences (related to: *Morpholino and mRNA Injection*)

Gene	Morpholino sequence	Reference
vhl	GGCATCGTCAAAGACAGGACAGTTC	(Harris et al., 2013)
hif1ab	ACCCTACAAAAGAAAGAAGGAGAGC	(Mendelsohn et al., 2008)
pdgfrb	ACAGGAACTGAAGTCACTGACCTTC	(Wiens et al., 2010)
il6	AAACCAGTATATAACAGCACCTGCT	*not previously published*

Supplemental Methods Table 2: Primer Sequences (related to: *Quantitative RT-PCR*)

Gene	Forward	Reverse	Reference
tbp	CGGTGGATCCTGCGAATTA	TGACAGGTTATGAAGCAAAACA ACA	(McCurley and Callard, 2008)
runx1	CGTCTTCACAAACCCTCCTCAA	GCTTTACTGCTTCATCCGGCT	(Harris et al., 2013)
cmyb	TGATGCTTCCCAACACAGAG	TTCAGAGGGAATCGTCTGCT	(Harris et al., 2013)
gp130	TTGATGTGTGAAGCCTCCAG	TGGGTCTCTCAATCCTGGTT	
il6	TCCCCGTGTTCAGCAGTATG	GCGGTCTGAAGGTTTGAGGA	
il6R	TGGCTGTATGTGTCTTGTGC	TGGCTGAACAGGAAGGAAGT	
pdgfba	GGACCCTCTTCCTCCATCTC	TGGGACACGTAACTGACAGC	(Harris et al., 2013)
pdgfbb	CAAGACCCTGCAGTGTGTTC	CACGTGCGTCTAGTTTCTGG	
pdgfaa	AAACAAGGCCACCATAAGGA	GCTGTTGGATCCACCTGACT	
pdgfrb	ACACACCGGGGTTTATGTGT	TATTGATGGGTTCGTCACCA	
pdgfra	GCTCATGATGAAGTGCTGGA	TCATCAAAGCCACTCTCACG	
stat3	GCAGGAGAACAACGTCCTGT	TGATGTCCTGCAGGTTGTGT	
mmp2	GCTGTTCCCGATGACCTAGA	GCTGTCATTTCTGGCCATTT	
mmp9	TCATGATCTCTGCGAAGTGG	TTGCCTTTTCCTCTCTGCAT	
b-actin	TCTGTCCCA TGCCAACCA T	TGCCCTCGTGCTGTTTT	(Harris et al., 2013)

SUPPLEMENTAL METHODS CITATIONS:

Harris, J.M., Esain, V., Frechette, G.M., Harris, L.J., Cox, A.G., Cortes, M., Garnaas, M.K., Carroll, K.J., Cutting, C.C., Khan, T.*, et al.* (2013). Glucose metabolism impacts the spatiotemporal onset and magnitude of HSC induction in vivo. Blood *121*, 2483-2493.

McCurley, A.T., and Callard, G.V. (2008). Characterization of housekeeping genes in zebrafish: male-female differences and effects of tissue type, developmental stage and chemical treatment. BMC molecular biology *9*, 102.

Mendelsohn, B.A., Kassebaum, B.L., and Gitlin, J.D. (2008). The zebrafish embryo as a dynamic model of anoxia tolerance. Developmental dynamics : an official publication of the American Association of Anatomists *237*, 1780-1788.

Wiens, K.M., Lee, H.L., Shimada, H., Metcalf, A.E., Chao, M.Y., and Lien, C.L. (2010). Platelet-derived growth factor receptor beta is critical for zebrafish intersegmental vessel formation. PloS one *5*, e11324.

Figure S1.

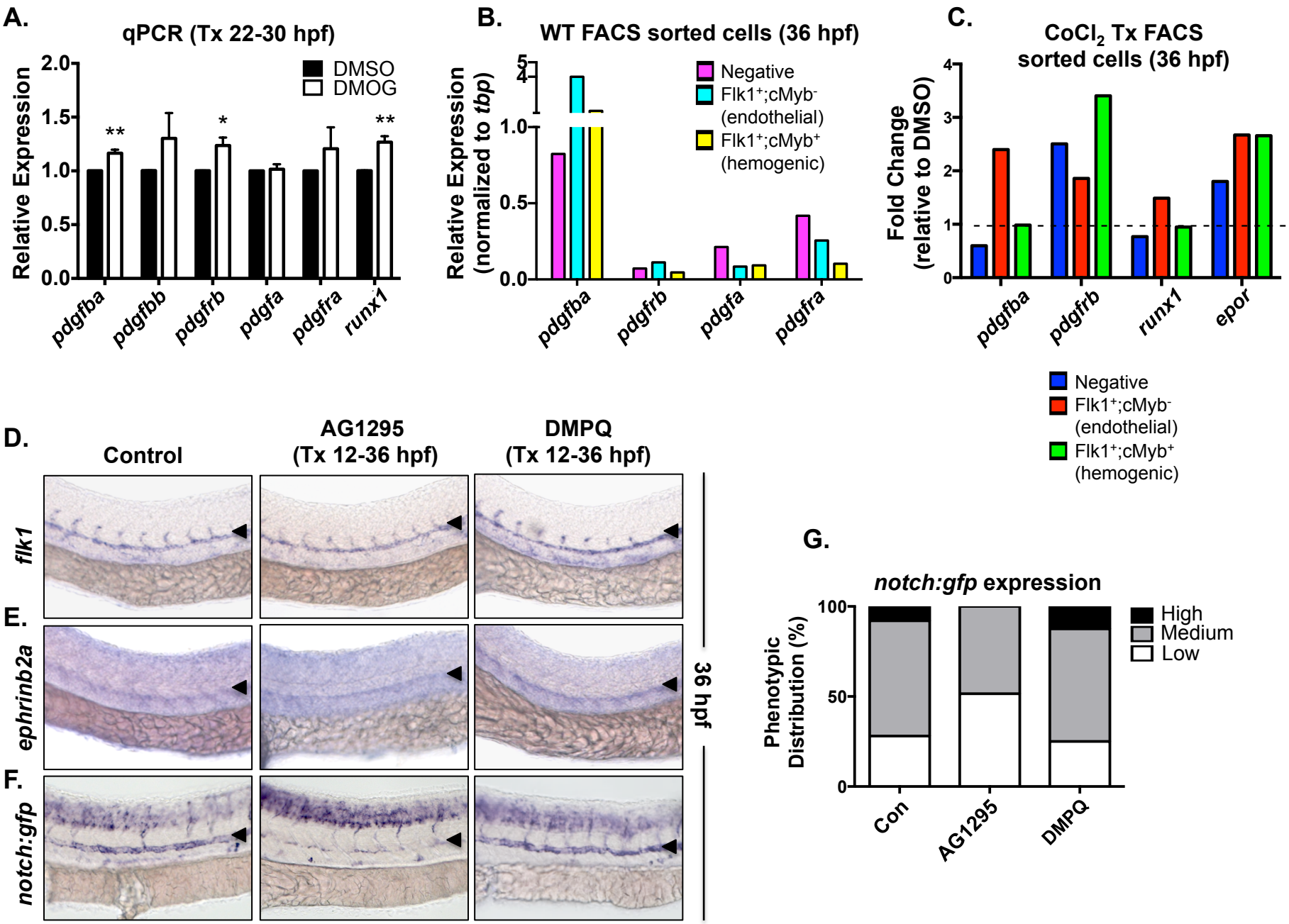
A.
qPCR (Tx 22-30 hpf)
Relative Expression
DMSO
DMOG
pdgfba
pdgfbb
pdgfrb
pdgfa
pdgfra
runx1
B.
WT FACS sorted cells (36 hpf)
Relative Expression (normalized to tbp)
Negative
Flk1+;cMyb- (endothelial)
Flk1+;cMyb+ (hemogenic)
C.
CoCl2 Tx FACS sorted cells (36 hpf)
Fold Change (relative to DMSO)
epor
D.
Control
AG1295 (Tx 12-36 hpf)
DMPQ (Tx 12-36 hpf)
flk1
E.
ephrinb2a
F.
notch:gfp
36 hpf
G.
notch:gfp expression
Phenotypic Distribution (%)
High
Medium
Low
Con
AG1295
DMPQ

Figure S2.

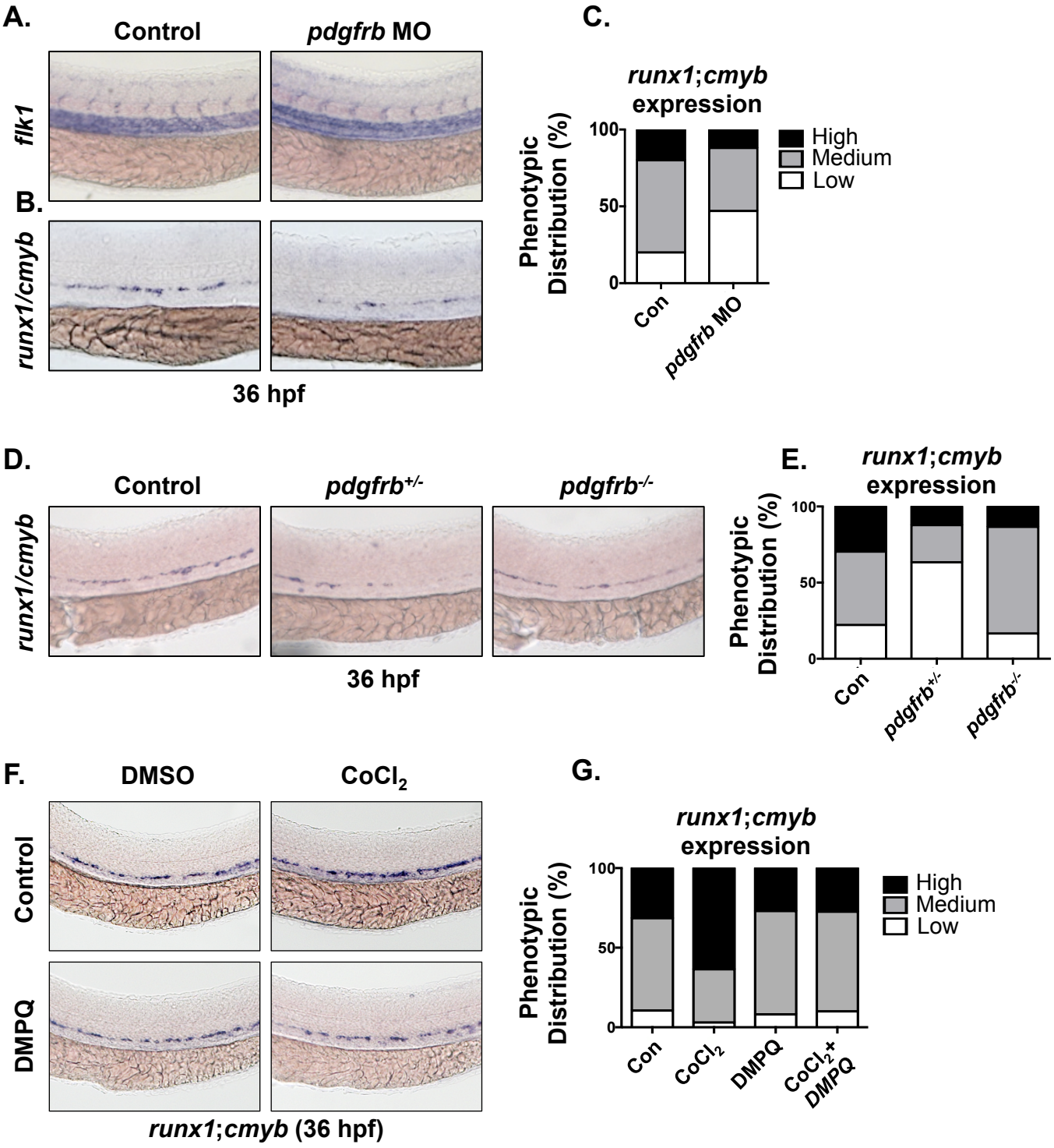
A.
Control
pdgfrb MO
flk1
B.
runx1/cmyb
36 hpf
C.
runx1;cmyb expression
Phenotypic Distribution (%)
100
50
0
High
Medium
Low
Con
pdgfrb MO
D.
Control
pdgfrb+/-
pdgfrb-/-
runx1/cmyb
36 hpf
E.
runx1;cmyb expression
Phenotypic Distribution (%)
100
50
0
Con
pdgfrb+/-
pdgfrb-/-
F.
DMSO
CoCl2
Control
DMPQ
runx1;cmyb (36 hpf)
G.
runx1;cmyb expression
Phenotypic Distribution (%)
100
50
0
High
Medium
Low
Con
CoCl2
DMPQ
CoCl2+ DMPQ

Figure S3.

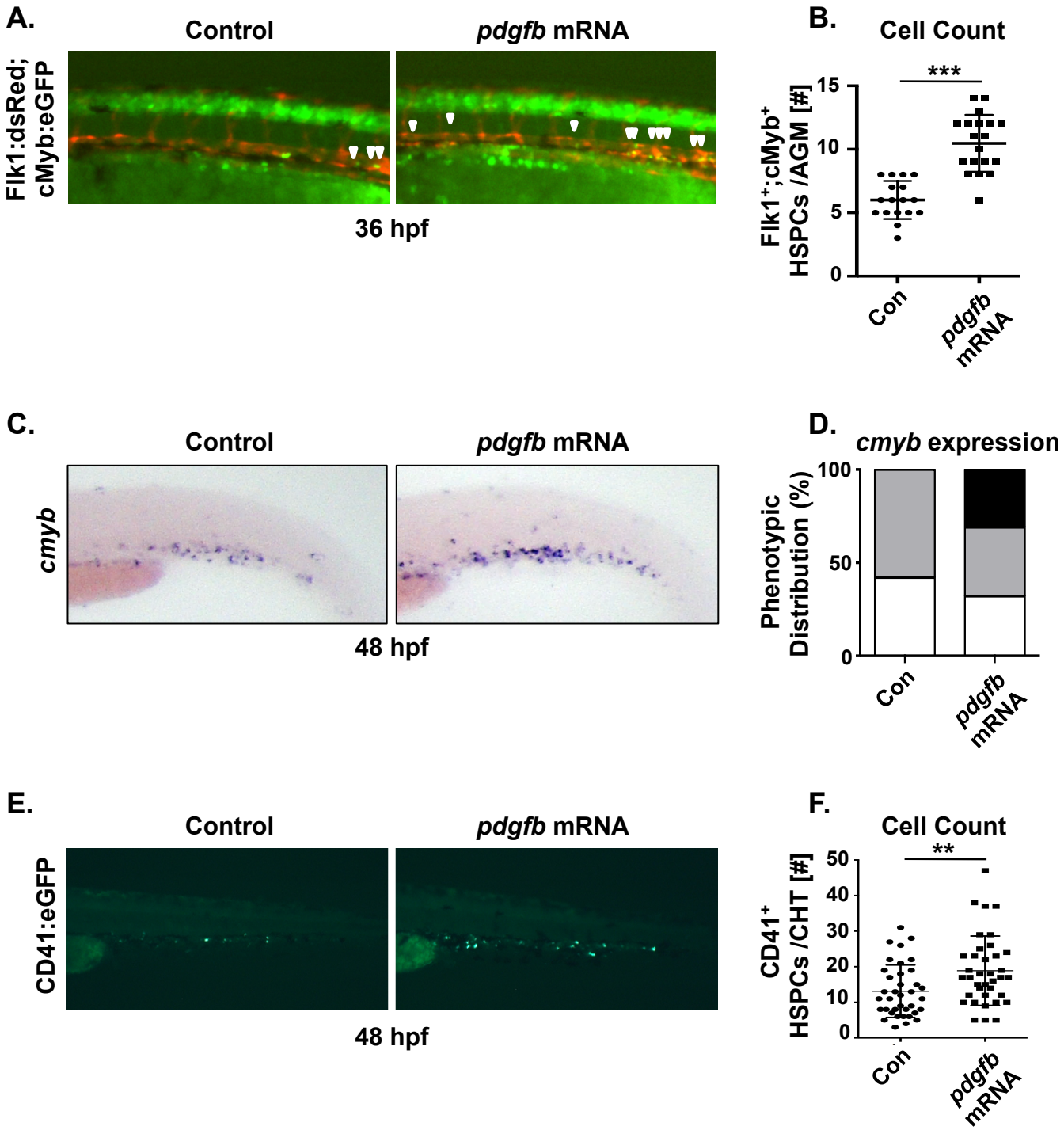
A.
Control
pdgfb mRNA
Flk1:dsRed; cMyb:eGFP
36 hpf
B.
Cell Count
***
Flk1+;cMyb+ HSPCs /AGM [#]
15
10
5
0
Con
pdgfb mRNA
C.
Control
pdgfb mRNA
cmyb
48 hpf
D.
cmyb expression
Phenotypic Distribution (%)
100
50
0
Con
pdgfb mRNA
E.
Control
pdgfb mRNA
CD41:eGFP
48 hpf
F.
Cell Count
**
CD41+ HSPCs /CHT [#]
50
40
30
20
10
0
Con
pdgfb mRNA

Figure S4.

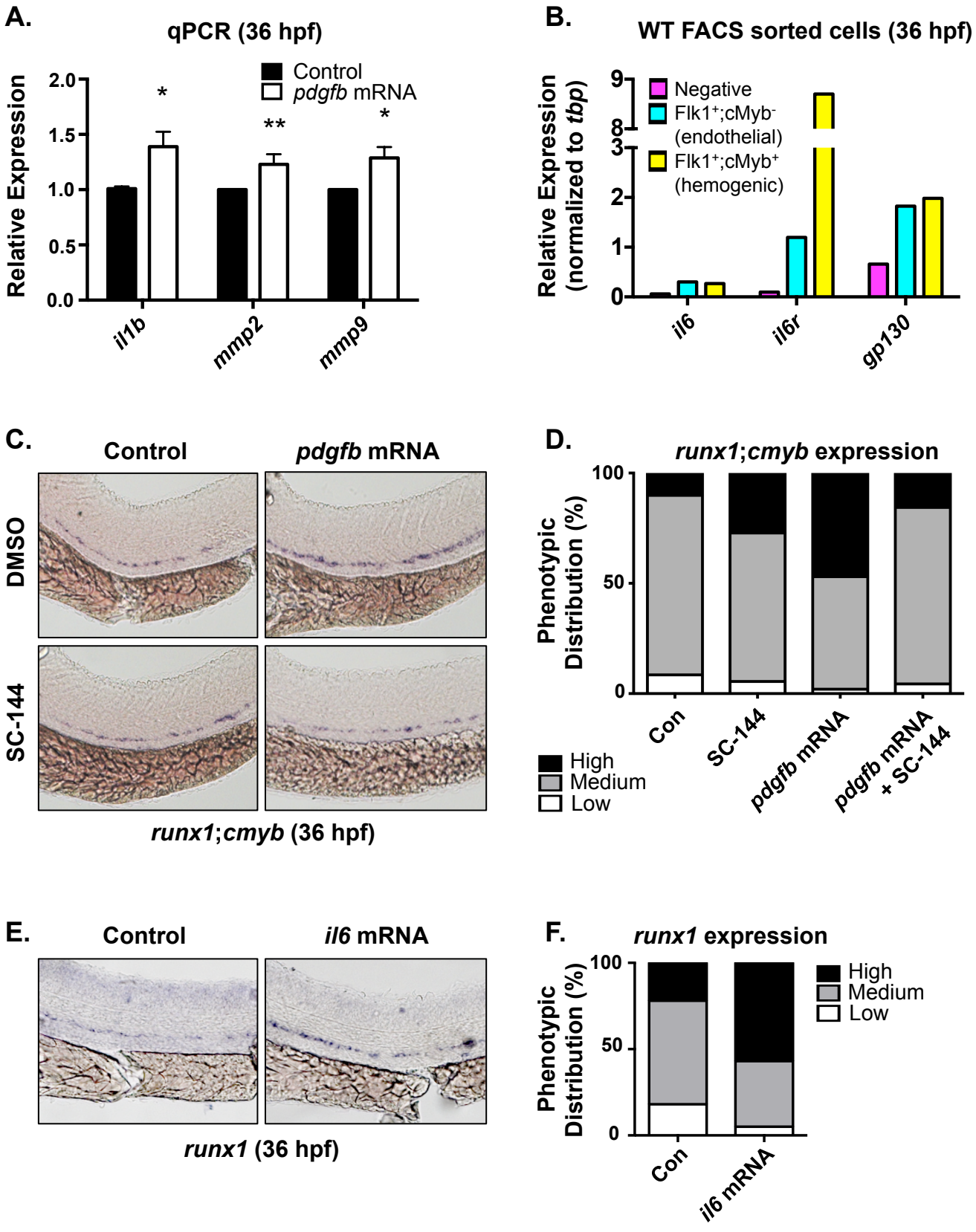
A.
qPCR (36 hpf)
Relative Expression
Control
pdgfb mRNA
2.0
1.5
1.0
0.5
0.0
*
**
*
il1b
mmp2
mmp9
B.
WT FACS sorted cells (36 hpf)
Relative Expression (normalized to tbp)
Negative
Flk1+;cMyb- (endothelial)
Flk1+;cMyb+ (hemogenic)
9
8
3
2
1
0
il6
il6r
gp130
C.
Control
pdgfb mRNA
DMSO
SC-144
runx1;cmyb (36 hpf)
D.
runx1;cmyb expression
Phenotypic Distribution (%)
100
50
0
Con
SC-144
pdgfb mRNA
pdgfb mRNA + SC-144
High
Medium
Low
E.
Control
il6 mRNA
runx1 (36 hpf)
F.
runx1 expression
Phenotypic Distribution (%)
100
50
0
Con
il6 mRNA
High
Medium
Low

Figure S5.

A.

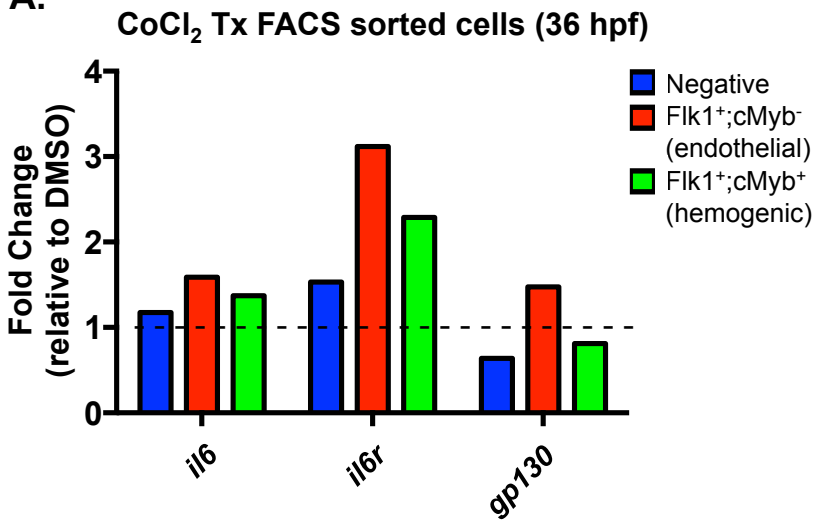

B.

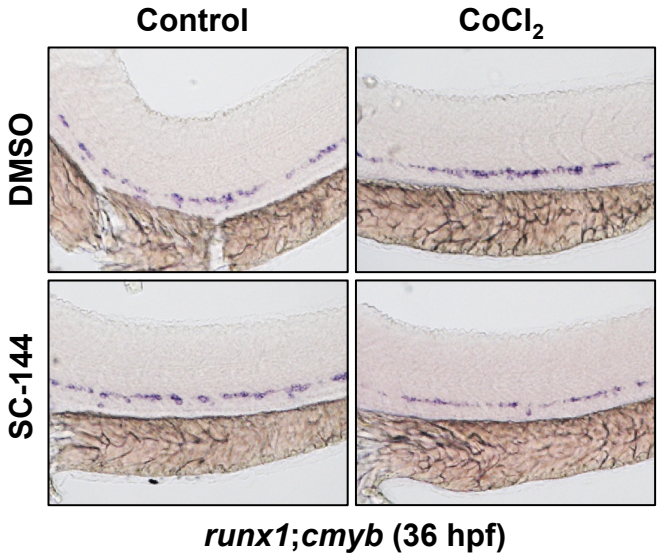

C.